Hydrosilylation with Bis(alkynyl)(1,5-cyclooctadiene)platinum Catalysts: A Density Functional Study of the Initial Activation

Mavinahalli N. Jagadeesh and Walter Thiel*

Max-Planck-Institut für Kohlenforschung, Kaiser-Wilhelm-Platz 1, D-45470 Mülheim an der Ruhr, Germany

Jutta Köhler

Consortium für elektrochemische Industrie GmbH, Zielstattstrasse 20, D-81379 München, Germany

Armin Fehn

Wacker-Chemie GmbH, Werk Burghausen, Johannes-Hess-Strasse 24, D-84480 Burghausen, Germany

Received January 9, 2002

At elevated temperatures bis(alkynyl)(1,5-cyclooctadiene)platinum complexes catalyze the cross-linking of polyorganosiloxanes containing Si−H and vinyl groups. Density functional calculations with medium-size basis sets and effective core potentials are reported for reactions that may activate these precatalysts for hydrosilylation. For a model system consisting of the bis(ethynyl) complex, trimethylsilane, and ethylene, the computations provide two plausible pathways for gaining access to the Chalk−Harrod cycle. The first one involves a sequence of four oxidative additions and reductive eliminations, while the second one requires a reductive coupling that is induced by olefin coordination. In both cases, the initial step is rate-determining, with a computed barrier of 27 kcal/mol. Experiments for polysiloxane systems of industrial interest favor the first pathway and yield barriers of 25−30 kcal/mol. Substituents in the alkynyl groups affect the measured barriers and the barriers computed for the rate-determining initial step of the first pathway in a qualitatively similar manner. We propose that the activation of the precatalysts is initiated by oxidative addition of Si−H.

Introduction

Hydrosilylation reactions involve the addition of hydrosilanes to unsaturated bonds.[1−4] Hydrosilylation of alkenes is one of the most important methods of forming silicon−carbon bonds and is therefore widely used for the synthesis of organosilicon compounds. In the silicone industry, this reaction is applied for making organofunctional silicon monomers and for cross-linking silicon polymers. Industrial products include silicone rubber, liquid injection molding compounds, paper release coatings, pressure sensitive adhesives, binders, and coupling agents.[1,5−7]

Hydrosilylation reactions are normally carried out under mild conditions in the presence of a catalyst.[1−4] A large variety of effective catalysts are available, most notably transition metal complexes of group VIII elements (Co, Rh, Ni, Pd, and Pt). The most commonly used catalysts are platinum compounds such as chloroplatinic acid in alcohol,[8] platinum(II) complexes with olefins, and platinum(0) complexes with phosphines.[1−4]

We are interested in a typical industrial application of hydrosilylation, namely, the construction of siloxane networks from organopolysiloxanes containing aliphatic C=C double bonds and Si−H bonds.[1,5−7] Addition curable silicone rubber compositions cross-link by hydrosilylation, which is normally catalyzed by small amounts of highly active platinum compounds (10−100 ppm). To avoid premature cross-linking, addition curing silicone compositions are generally handled as two-component systems consisting of the unsaturated polyorganosiloxane plus catalyst and the cross-linker with Si−H bonds.

(1) Marciniec, B.; Gulinski, J.; Urbaniak, W.; Kornetka, Z. W. *Comprehensive Handbook on Hydrosilylation*; Pergamon Press: Oxford, 1992.

(2) Ojima, I. In *The Chemistry of Organic Silicon Compounds*; Patai, S., Rappoport, Z., Eds.; John Wiley & Sons: New York, 1989; pp 1479−1526.

(3) Armitrage, D. A. In *Comprehensive Organometallic Chemistry*; Wilkinson, G., Stone, F. G. A., Abel, W. E., Eds.; Pergamon Press: Oxford, 1982; pp 117−120.

(4) Speier, J. L. In *Advances in Organometatallic Chemistry*; Stone, F. G. A., West, R., Eds.; Academic Press: New York, 1979; Vol. 17, pp 407−447.

(5) Lewis, L. N.; Stein, J.; Gao, Y.; Colborn, R. E.; Hutchins, G. *Platinum Met. Rev.* **1997**, *41,* 66−75.

(6) Stark, F. O.; Falender, J. R.; Wright, A. P. In *Comprehensive Organometallic Chemistry*; Wilkinson, G., Stone, F. G. A., Abel, W. E., Eds.; Pergamon Press: Oxford, 1982; Vol. 2, pp 306−362.

(7) Noll, W. *Chemistry and Technology of Silicones*; Academic Press: New York, 1968.

(8) (a) Speier, J. L.; Webster, J. A.; Barnes, G. H. *J. Am. Chem. Soc.* **1957**, *79*, 974. (b) Saam, J. C.; Speier, J. L. *J. Am. Chem. Soc.* **1958**, *80*, 4104. (c) Ryan, J. W.; Speier, J. L. *J. Am. Chem. Soc.* **1964**, *86*, 895.

10.1021/om0200196 CCC: $22.00
Publication on Web 04/18/2002

Prior to use, the two components must be mixed together in a well-defined ratio to initiate the cross-linking reaction which yields the desired silicone rubber material. A major disadvantage of such addition curing systems is the necessity to handle two separate components during the whole process from manufacturing and packaging to mixing.

Consequently there have been many attempts to provide an addition-cross-linking silicone material as a one-component formulation with an extended work life at ambient temperature and a rapid cure at elevated temperature. The central problem in the development of one-component systems is to suppress any premature cross-linking, which usually occurs already at room temperature in the presence of the platinum catalyst. One possible solution is the use of inhibitors[1,9,10] which can form complexes with the catalyst; this reduces its activity at room temperature considerably, but may also impair the activity at higher temperatures due to incomplete decomplexation, which may cause low cross-linking rates or even incomplete cure. A second approach is the encapsulation of the platinum catalyst in a finely divided material such as a thermoplastic silicone resin, an organic thermoplast, or a cyclodextrine,[1,11,12] which does not release the catalyst until a certain temperature is reached; problems with this approach include the large size of the capsules (preventing the formation of stable suspensions) and the sudden release of locally high catalyst doses (resulting in inhomogeneous cross-linking). A third method is the design of new classes of platinum catalysts that show essentially no hydrosilylation activity at ambient temperatures and high curing rates above a tunable kick-off temperature, thus combining pot lives of several months with high curing rates.[13] One of the best examples for such catalysts are bis(alkynyl)(1,5-cyclooctadiene)platinum complexes (COD)Pt(CCR)$_2$.[14]

For a rational optimization of these new platinum (pre)catalysts, it is essential to understand how they work and, in particular, how they are activated at higher temperatures. Given the complexity of the real systems that are used industrially, an experimental study of the underlying reaction mechanisms is difficult. We have therefore decided to investigate suitable model systems computationally using density functional theory in order to identify possible modes of reaction.

It is commonly accepted that the transition metal catalyzed hydrosilylation proceeds by the Chalk−Harrod mechanism.[15] Recent ab initio studies[16−19] of the bis(phosphine)platinum(0)-catalyzed hydrosilylation of ethylene by silane have covered the full Chalk−Harrod cycle (oxidative addition of SiH_4 to $Pt(PH_3)_2$, coordination of C_2H_4, ethylene insertion into Pt−H, and reductive elimination of $H_3Si-C_2H_5$). They have provided much detailed insight into these reactions and have shown in particular that the Chalk−Harrod cycle is energetically feasible (with a maximum barrier of about 22 kcal/mol) and preferred over a modified Chalk−Harrod cycle with ethylene insertion into the Pt−Si bond even if cis−trans isomerization of the intermediates is taken into account.[16−18]

The present paper investigates possible initial transformations of the (pre)catalyst (COD)Pt(CCR)$_2$ that allow access to the Chalk−Harrod cycle. The next section describes the computational methods used. In the following sections, we report the theoretical results and discuss them in the context of the available experimental evidence.

Computational Methods

The quantum-chemical calculations were carried out using density functional theory (DFT).[20] They employed the gradient-corrected BP86 functional which combines the Becke exchange[21] and Perdew correlation[22] functionals. For platinum we used a small-core quasirelativistic effective core potential with the associate (8s7p6d)/[6s5p3d] valence basis set contracted according to a (311111/22111/411) scheme.[23] The other elements were represented by the 6-31G(d) basis[24] with one set of d polarization functions at all non-hydrogen atoms. Spherical d functions were used throughout. Unless noted otherwise, geometries were optimized without symmetry constraints. Transition states were normally located using the synchronous transit-guided quasi-Newton (STQN) method.[25] Force constants were computed for all stationary points to establish their character. All calculations were performed using the Gaussian98 program.[26]

Results

In our computational studies, the precatalyst is represented by the parent (1,5-cyclooctadiene)bis(ethynyl)platinum complex (COD)Pt(CCH)$_2$, and the reactants are modeled by trimethylsilane, $HSiMe_3$, and ethylene, C_2H_4. This is clearly a severe simplification of the real system, which contains a substituted precatalyst (COD)Pt(CCR)$_2$ (where R is normally aryl) and

(9) Examples of inhibitors from the patent literature: (a) Hatanaka, M.; Kurita, A. U.S. Pat. 4,329,275, 1982. (b) Sasaki, S.; Hamada, Y. U.S. Pat. 4,603,168, 1986. (c) Michel, U.; Delker, J. R. U.S. Pat. 4,530,989, 1985. (d) Shirahata, A.; Shosaku, S. U.S. Pat. 4,465,818, 1984. (e) Cavezzan, J. U.S. Pat. 4,595,739 (1986). (f) Kniege, W.; Michel, W.; Ackerman, J.; Randolph, K. H. U.S. Pat. 4,487,906, 1984. (g) Janik, G.; Buentello, M. U.S. Pat. 4,487,906, 1984. (h) Lo, P. Y. K. U.S. Pat. 4,774,111, 1988.

(10) Examples of recent work on inhibitors: (a) Kishi, K.; Ishimaru, T.; Ozono, M.; Tomita, I.; Endo, T. *J. Polym. Sci. A: Polym. Chem.* **2000**, *38*, 35−42. (b) Kishi, K.; Ishimaru, T.; Ozono, M.; Tomita, I.; Endo, T. J. *Polym. Sci. A: Polym. Chem.* **2000**, *38*, 804−809.

(11) Examples of encapsulation from the patent literature: (a) Togashi, A.; Kasuya, A. Eur. Pat. Appl. 449,181, 1991. (b) Fujioka, K.; Yashida, Y. U.S. Pat. 5, 525,425, 1996.

(12) (a) Lewis, L. N.; Sumpter, C. A.; Davis, M. *J. Inorg. Organomet. Polym.* **1995**, *5*, 377−390. (b) Lewis, L. N.; Sumpter, C. A.; Stein, J. *J. Inorg. Organomet. Polym.* **1996**, *6*, 123−144.

(13) (a) Sumpter, C. A.; Lewis, L. N.; Lawrence, N. B. U.S. Pat. 5,331,075, 1994. (b) Fehn, A.; Achenbach, F.; Dietl, S. U.S. Pat. 6,-187,890, 2001.

(14) Fehn, A.; Achenbach, F. Eur. Pat. Appl. 994,159, 2000.

(15) Chalk, A. J.; Harrod, J. F. *J. Am. Chem. Soc.* **1965**, *87*, 16−21.

(16) Sakaki, S.; Mizoe, N.; Sugimoto, M. *Organometallics* **1998**, *17*, 2510−2523.

(17) Sakaki, S.; Mizoe, N.; Musashi, Y.; Sugimoto, M. *J. Mol. Struct. (THEOCHEM)* **1999**, *462*, 533−546.

(18) Sakaki, S.; Mizoe, N.; Sugimoto, M.; Musashi, Y *Coord. Chem. Rev.* **1999**, *192*, 933−960.

(19) Sugimoto, M.; Yamasaki, I.; Mizoe, N.; Antai, M.; Sakaki, S. *Theor. Chem. Acc.* **1999**, *102*, 377−384.

(20) Parr, R. G.; Yang, W. *Density Functional Theory of Atoms and Molecules*; Oxford University Press: Oxford, 1989.

(21) Becke, A. D. *Phys. Rev. A* **1988**, *38*, 3098−3100.

(22) Perdew, J. P. *Phys. Rev. B* **1986**, *33*, 8822−8824.

(23) Andrae, D.; Häussermann, U.; Dolg, M.; Stoll, H. *Theor. Chim. Acta* **1990**, *77*, 123−141.

(24) (a) Hehre, W. J.; Ditchfield, R.; Pople, J. A. *J. Chem. Phys.* **1972**, *56*, 2257−2261. (b) Hariharan, P. C.; Pople, J. A. *Theor. Chim. Acta* **1973**, *28*, 213−222. (c) Francl, M. M.; Pietro, W. J.; Hehre, W. J.; Binkley, J. S.; Gordon, M. S.; DeFrees, D. J.; Pople, J. A. *J. Chem. Phys.* **1982**, *77*, 3654−3665.

(25) (a) Peng, C. Y.; Schlegel, H. B. *Isr. J. Chem.* **1994**, *33*, 449−454. (b) Peng, C. Y.; Ayala, P. Y.; Schlegel, H. B. *J. Comput. Chem.* **1996**, *17*, 49−56.

Scheme 1. Chalk−Harrod Mechanism

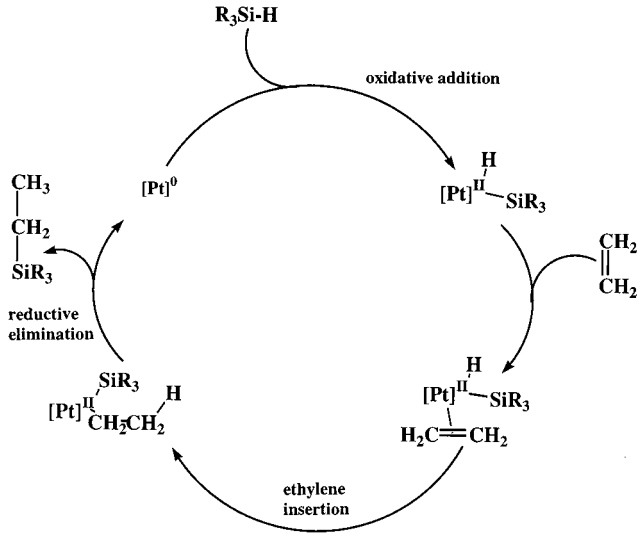

polyorganosiloxane reactants with Si−H bonds and vinyl groups. We expect, however, that the DFT calculations on the model system will still be helpful to assess the intrinsic reactivities in the real system.

Scheme 1 depicts the Chalk−Harrod mechanism[15] for the platinum-catalyzed hydrosilylation of alkenes. After oxidative addition of the silane and coordination of the alkene, three coordination sites at platinum are occupied by the reactants. Assuming that platinum can provide at most six coordination sites, the active catalytic species can accommodate other ligands at no more than three sites. Since the bis(alkynyl)(1,5-cyclooctadiene)platinum complexes (COD)Pt$(CCR)_2$ are tetracoordinated, it is obvious that some decoordination is required for the activation of the precatalyst.

The most direct path from the precatalyst to the Chalk−Harrod cycle would involve decoordination of 1,5-cyclooctadiene (COD) or reductive elimination of diacetylene to yield dicoordinated platinum complexes. These reactions are computed to be endothermic by 61 and 45 kcal/mol, respectively, and can therefore be ruled out. Hence we need to consider more complicated pathways involving interactions between the precatalyst and the reactants.

Scheme 2 shows a possible conversion of the precatalyst **1** by oxidative addition of trimethylsilane to yield the hexacoordinated adduct **2**, which may then be transformed to the tetracoordinated species **8** either directly by reductive coupling (elimination of diacetylene) or by a three-step sequence of reductive elimination ($HCCSiMe_3$ or HCCH), oxidative addition ($HSiMe_3$), and reductive elimination (HCCH or $HCCSiMe_3$). Species **8** can enter the Chalk−Harrod cycle (see Scheme 1). The hydrogen migration from Pt to COD has been considered as a side reaction of intermediate **2** which leads to **5**.

Scheme 3 outlines an alternative conversion of the precatalyst **1** that starts with the decoordination of one COD double bond to yield the tricoordinated species **9**. This species can formally undergo a large number of reactions. It turns out, however, that **9** is relatively high in energy, and we have thus only considered the oxidative addition of trimethylsilane leading to **10** and the loss of COD from **9** and **10**.

Scheme 4 shows another conceivable pathway that involves the initial addition of ethylene to the precatalyst **1**. The resulting π complex **11** may then undergo reductive elimination of diacetylene to yield compound **12**, followed by an oxidative addition of trimethylsilane. The complex **13** thus formed is an entry point to the Chalk−Harrod cycle (see Scheme 1) and can rearrange to **14** by ethylene insertion.

We have carried out DFT calculations on most of the reactions in Schemes 2−4. The platinum complexes studied are collected in Scheme 5 for easy reference. Total energies and zero-point vibrational energies of all species considered are given as Supporting Information. Table 1 lists the relevant reaction and activation energies. Figures 1−3 present reaction profiles for the pathways investigated, while Figures 4−11 show the most important transition structures (others being available as Supporting Information, Figures S1−S4). Table 2 contains selected geometrical parameters of the optimized minimum structures. In the following we shall discuss the theoretical results in the order suggested by the reaction sequences in Schemes 2−4. Since the relative energies without and with zero-point vibrational corrections do not differ much (see Table 1), we shall only quote the former in the text.

The precatalyst **1** (C_2 symmetry) contains two σ-bonded ethynyl ligands (Pt−C bond length of 1.97 Å) and an η^4-COD ligand with two π bonds (Pt−C 2.25−2.28 Å, C=C 1.40 Å). Oxidative addition of $HSiMe_3$ (see Scheme 2) leads to a hexacoordinated species **2** with the silyl and one ethynyl group trans to the COD double bonds, while the hydride and the other ethynyl group occupy the remaining two coordination sites; hence the two ethynyl groups remain cis to each other in **2**, and the bulky $SiMe_3$ ligand points away from COD. The alternative addition product **2a**, with reversed positions of the H and $SiMe_3$ ligands, is less stable than **2** by 12.0 kcal/mol due to unfavorable steric interactions between $SiMe_3$ and COD. There are two further isomers **2b** and **2c** with a trans-arrangement of the ethynyl groups (energies of -4.5 and 15.3 kcal/mol relative to **2** depending on the position of $SiMe_3$) which are irrelevant for our purposes since they cannot be reached easily from the *cis*-bis(ethynyl) precatalyst **1**. The structures of **2** and its isomers **2a**−**c** (see Table 2) provide clear evidence of the trans-influence (structural trans-effect) which increases in the order ethynyl < hydride < $SiMe_3$:[27,28] for example, the Pt−C distances to the COD double bonds increase from 2.27−2.32 Å (trans to CCH) via

(26) Frisch, M. J.; Trucks, G. W.; Schlegel, H. B.; Scuseria, G. E.; Robb, M. A.; Cheeseman, J. R.; Zakrzewski, V. G.; Montgomery, J. A., Jr.; Stratmann, R. E.; Burant, J. C.; Dapprich, S.; Millam, J. M.; Daniels, A. D.; Kudin, K. N.; Strain, M. C.; Farkas, O.; Tomasi, J.; Barone, V.; Cossi, M.; Cammi, R.; Mennucci, B.; Pomelli, C.; Adamo, C.; Clifford, S.; Ochterski, J.; Petersson, G. A.; Ayala, P. Y.; Cui, Q.; Morokuma, K.; Malick, D. K.; Rabuck, A. D.; Raghavachari, K.; Foresman, J. B.; Cioslowski, J.; Ortiz, J. V.; Stefanov, B. B.; Liu, G.; Liashenko, A.; Piskorz, P.; Komaromi, I.; Gomperts, R.; Martin, R. L.; Fox, D. J.; Keith, T.; Al-Laham, M. A.; Peng, C. Y.; Nanayakkara, A.; Gonzalez, C.; Challacombe, M.; Gill, P. M. W.; Johnson, B. G.; Chen, W.; Wong, M. W.; Andres, J. L.; Head-Gordon, M.; Replogle, E. S.; Pople, J. A. *Gaussian 98*, revision A.7 and A.9; Gaussian, Inc.: Pittsburgh, PA, 1998.

(27) Coe, B. J.; Glenwright, S. J. *Coord. Chem. Rev.* **2000**, *203*, 5−80.

(28) Belluco, U. *Organometallic and Coordination Chemistry of Platinum*; Academic Press: New York, 1974.

Scheme 2. Conversion of Precatalyst by Oxidative Addition of $HSiMe_3$ and Subsequent Reactions

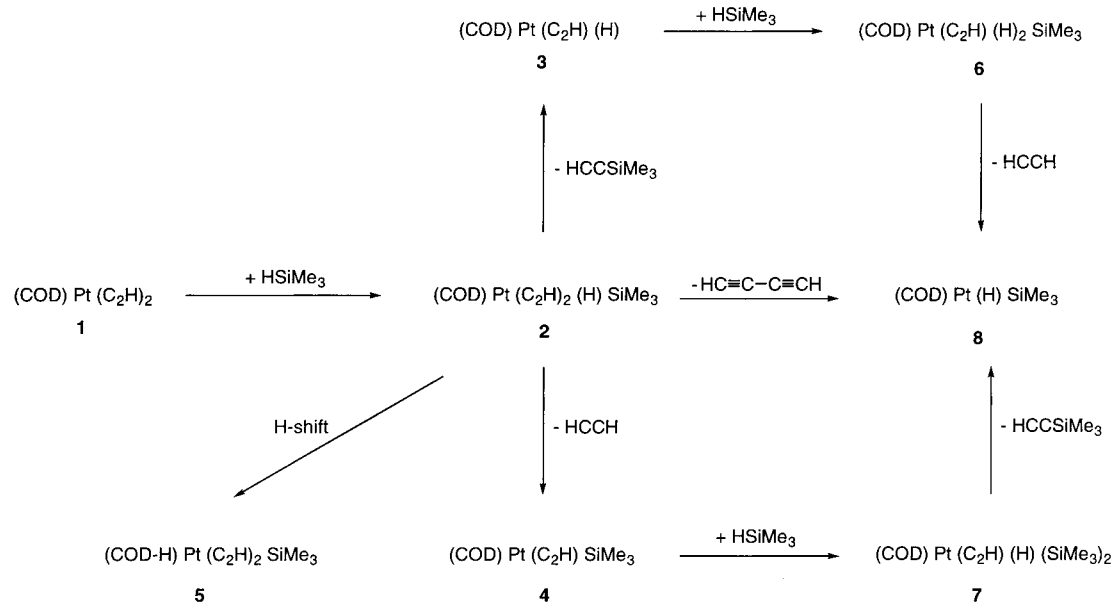

Scheme 3. Conversion of Precatalyst by Diene Decoordination and Subsequent Reactions

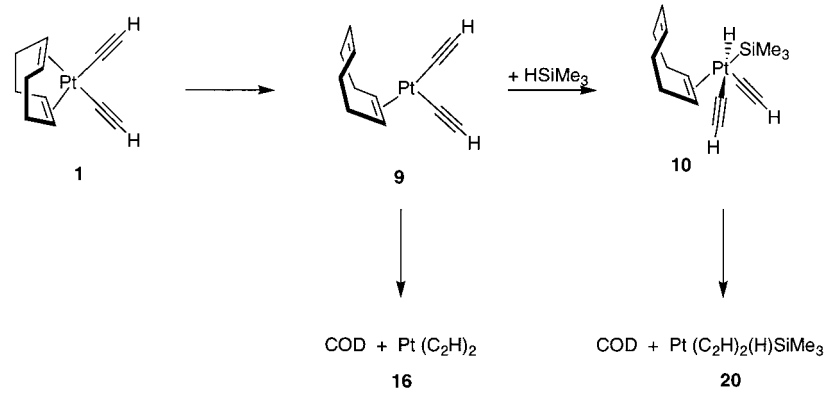

Scheme 4. Conversion of Precatalyst by Olefin Coordination and Subsequent Reactions

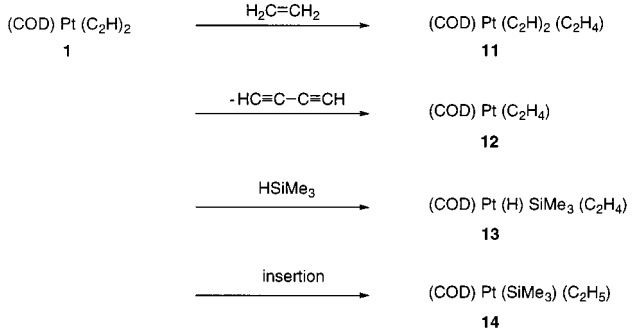

2.36−2.49 Å (trans to H) to 2.59−2.79 Å (trans to $SiMe_3$), with similar trends in the other Pt−ligand bond lengths.

The oxidative addition of $HSiMe_3$ to **1** is endothermic by 12 kcal/mol and has to overcome a barrier of 27 kcal/mol. The corresponding transition structure is already rather product-like (see Figure 4). The Pt−Si and Pt−H distances are only slightly larger than in **2** (2.67 vs 2.43 Å and 1.71 vs 1.62 Å, respectively), whereas the Si−H distance is elongated more strongly compared with $HSiMe_3$ (1.81 vs 1.51 Å). On the other hand, the trans-influence of $SiMe_3$ is not yet very pronounced in the transition structure (maximum Pt−C distance of 2.35 Å to the COD double bonds).

The initial adduct **2** can undergo at least four exothermic reactions (see Scheme 2). Reductive elimination of trimethylsilylacetylene $HCCSiMe_3$ leads to the most stable product **3** (20 kcal/mol below **2**), while the elimination of acetylene HCCH to yield **4** is somewhat less exothermic (by 14 kcal/mol). The barriers for these two eliminations are quite low (13−14 kcal/mol), and the corresponding transition states are almost isoenergetic with the transition state for the initial oxidative addition (slightly lower, see Figure 1). Both transition structures resemble **2**. This holds true particularly for the elimination of HCCH (see Figure 5), where the breaking Pt−H and Pt−C bonds show only minor elongations (by 0.10 and 0.07 Å, respectively), while the other Pt−ligand distances remain almost unchanged (forming C−H bond: 1.41 Å). The transition structure for elimination of $HCCSiMe_3$ (see Figure 6) deviates somewhat more from **2**, especially with regard to the weaker interactions with one of the COD double bonds, but the breaking Pt−Si and Pt−C bonds are again not much longer than in **2** (by 0.24 and 0.03 Å, respectively), and the SiCC angle of 127° is still far from linearity (forming Si−C bond: 2.10 Å).

Scheme 5. Platinum Complexes Studied

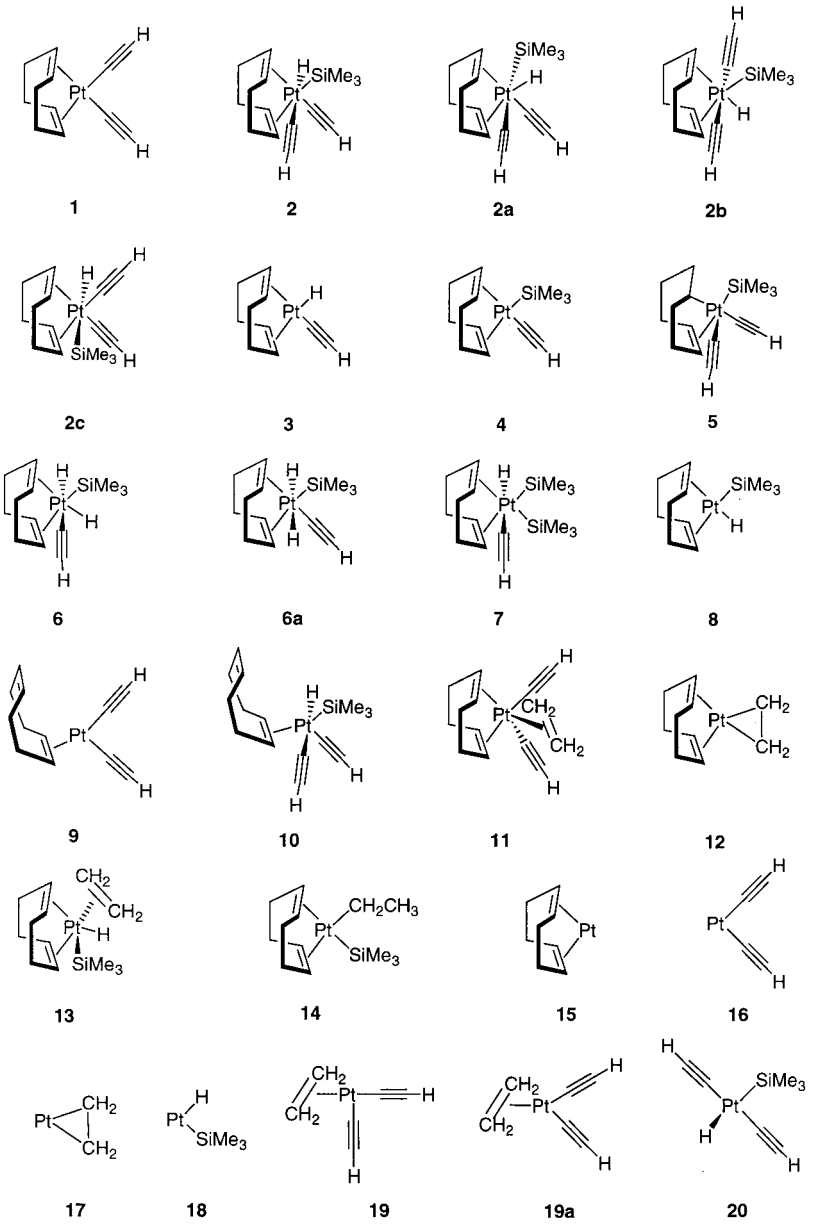

The elimination products **3** and **4** can be converted to the tetracoordinated species **8** by oxidative addition of $HSiMe_3$ and subsequent elimination of HCCH or $HCCSiMe_3$, respectively (see Scheme 2). The pathway **3** → **8** should be favored since it starts from the more stable compound and avoids the destabilization from steric hindrance that is expected to occur between the two bulky $SiMe_3$ ligands on the alternative pathway **4** → **8**. On the first route, the intermediate *cis*-dihydride **6** is more stable than the corresponding *trans*-dihydride **6a**, while the complex **7** with two $SiMe_3$ groups trans to COD is the lowest intermediate on the second route (see Schemes 2 and 5). Relative to a common reference system (**2** + $HSiMe_3$), the energies of the intermediates increase in the order **6** < **6a** < **7** (i.e., −16 < −11 < −6 kcal/mol). Hence, as expected on steric grounds, the pathway **3** → **8** is strongly favored already at the level of the intermediates (by 10 kcal/mol), and we have therefore located transition states only for this transformation. The oxidative addition of $HSiMe_3$ to **3** may proceed in two orientations, with barriers of 17 and 22 kcal/mol, and the resulting adducts **6** and **6a** can eliminate HCCH easily, with barriers of 18 and 16 kcal/mol, respectively. The alternative reductive eliminations of $HCCSiMe_3$ from **6** and **6a** should have similar barriers (see the results for **2**), but they do not provide direct access to the Chalk−Harrod cycle and were therefore not studied. The overall conversion **3** → **8** is endothermic by 3 kcal/mol and requires an activation of 22 kcal/mol via **6** (or 24 kcal/mol via **6a**). It is facile in the sense that each transition state is energetically far below the initial transition state for **1** → **2** (see Figure 2).

This is not true for the other two transformations of the initial adduct **2** (see Scheme 2), which have to overcome larger barriers, i.e., 21 kcal/mol for the rearrangement **2** → **5** by hydrogen migration from Pt to COD and 25 kcal/mol for the direct one-step conversion **2** → **8** by reductive elimination of diacetylene. The transition structure for the latter reaction (see Figure 7) is reactant-like since the coordination geometry of the remaining ligands (COD, H, and $SiMe_3$) is similar to

Table 1. Calculated Reaction Energies and Activation Energies (kcal/mol)[a]

reaction[b]	ΔE	ΔE_0	$\Delta E^{\ddagger}$	$\Delta E_0^{\ddagger}$
1 + $HSiMe_3$ → **2**	11.8	13.1	26.8	26.7
2 → **3** + $HCCSiMe_3$	−19.9	−21.1	13.4	12.1
2 → **4** + HCCH	−14.1	−15.5	14.0	11.5
2 → **5**	−10.1	−8.7	21.4	20.3
2 → **8** + HCCCCH	−16.8	−18.4	24.6	22.7
3 + $HSiMe_3$ → **6**	3.9	5.1	17.0	17.5
3 + $HSiMe_3$ → **6a**	8.5	9.3	22.3	22.1
4 + $HSiMe_3$ → **7**	7.8	9.3		
6 → **8** + HCCH	−0.8	−2.4	17.8	15.1
6a → **8** + HCCH	−5.4	−6.6	15.4	13.1
7 → **8** + $HCCSiMe_3$	−10.6	−12.2		
1 → **9**	37.7	36.2	40.0	38.2
9 → **10**	−9.5	−7.7		
9 → **16** + COD	23.5	22.4		
1 + C_2H_4 → **11**	12.0	14.3	13.1	14.8
11 → **12** + HCCCCH	−21.9	−23.2	14.4	13.1
12 + $HSiMe_3$ → **13**	5.6	7.0	12.1	13.1
13 → **14**	−19.9	−17.8		

[a] Computed from the energies given in Table S1 of Supporting Information; reaction energies ΔE and activation energies $\Delta E^{\ddagger}$ refer to total energies without zero-point vibrational corrections, while ΔE_0 and $\Delta E_0^{\ddagger}$ include these corrections. [b] See Schemes 2−4.

that in **2**. The breaking Pt−C bonds are only slightly longer than in **2** (by 0.02−0.05 Å), but the leaving ethynyl groups have moved much closer together to initiate the formation of the new central bond in diacetylene (C−C 1.75 Å).

Summarizing the results for Scheme 2, we have found a feasible four-step path **1** → **2** → **3** → **6** → **8** that converts the precatalyst (COD)$Pt(CCH)_2$ to the tetracoordinated species (COD)$Pt(H)SiMe_3$, which can enter the Chalk−Harrod cycle. This path involves an alternating sequence of oxidative additions ($HSiMe_3$) and reductive eliminations ($HCCSiMe_3$, HCCH). The rate-determining step is the initial oxidative addition **1** → **2** with a barrier of 27 kcal/mol.

We have also considered transformations of the precatalyst **1** that start with the decoordination of one COD double bond (see Scheme 3). The resulting tricoordinated species **9** contains a twisted COD ligand and is 38 kcal/mol less stable than **1**. It is separated from **1** by a small barrier of 2 kcal/mol and can therefore revert to **1** easily. The barrier for decoordination **1** → **9** thus amounts to 40 kcal/mol. As expected from the Hammond postulate, the transition structure (see Figure 8) resembles the product **9**, with two short Pt−C distances to the COD double bonds (2.26 Å, 2.35 Å) and two long ones (3.32 Å, 3.57 Å).

Full decoordination of COD from **9** is endothermic by another 23 kcal/mol and therefore energetically prohibitive (products 61 kcal/mol above **1**). We have checked oxidative addition of $HSiMe_3$ to **9** as an alternative pathway and found a corresponding adduct **10**, which is analogous to **2** in the orientation of the ligands (except that one of the COD double bonds is not coordinated). We could not locate the transition state for the reaction **9** → **10**, but exploratory calculations indicate that the barrier must be sizable (see also reaction **1** → **2**). Hence, we expect that the overall conversion **1** → **9** → **10** should require a larger activation than the value of 40 kcal/mol obtained for the first step. This is a moot issue, however, since the adduct **10** can also be reached via the path **1** → **2** → **10**, with a barrier of 27 kcal/mol for the first step (see above). Energetically, **10** lies above **1** and **2** (by 28 and 16 kcal/mol, respectively), and it must be separated from **2** at least by a small barrier (given the fact that it could be located by an unconstrained energy minimization). Likewise, loss of COD from **10** must require some activation. This latter reaction is exothermic by 6 kcal/mol and yields $Pt(CCH)_2(H)SiMe_3$ (a tetracoordinated complex **20** which could be a suitable entry into a Chalk−Harrod cycle). Concerning the overall conversion **1** → **2** → **10** → **20** the second or third step must be rate-determining since **10** is energetically already slightly above the transition state for the first step. We have not located the transition states for the second and third step, but we would assume on the basis of the data for related reactions that the overall barrier for the three-step conversion will be well over 30 kcal/mol.

Hence, the reactions in Scheme 3 should not be relevant mechanistically. Compared with the rate-limiting barrier of 27 kcal/mol for Scheme 2, the intermediate species **9** is significantly higher in energy (at 38 kcal/mol), and alternative pathways via **10** are also expected to be less favorable.

We now turn to reactions that might be initiated by interactions between the precatalyst and ethylene (see Scheme 4). It is experimentally known in nickel chemistry that olefins with electron-withdrawing substituents activate dialkyl(dipyridyl)nickel complexes to undergo reductive coupling, which yields the corresponding olefin complexes and alkanes.[29] A number of such reactions have been reported,[30] and there is both experimental and theoretical evidence that they proceed by an associative mechanism via pentacoordinated olefin complexes.[29,31] We have therefore studied the analogous reaction between our platinum-based precatalyst and ethylene.

Initially a weak van der Waals complex is formed between **1** and ethylene, with Pt−C distances to ethylene of more than 4 Å and a binding energy of less than 1 kcal/mol (see Figure 3). Closer approach of the ethylene leads to the formation of the π complex **11**, which lies in a very shallow minimum (12 kcal/mol above the reactants) and can dissociate again easily (barrier of 1 kcal/mol). The corresponding transition structure (see Figure 9) looks like the π complex, except that the Pt−C distances to the incoming ethylene are elongated by about 0.2 Å. Reductive elimination of diacetylene from the π complex requires an additional activation of 14 kcal/mol (i.e., 26 kcal/mol relative to the separated reactants). The transition structure (see Figure 10) differs from the π complex **11** mainly with regard to the ethynyl moieties: the breaking Pt−C bonds are still quite short (2.02 and 2.09 Å), but the two ethynyl ligands have approached each other to allow for the formation of the new central bond in diacetylene (C−C 1.83 Å).

The reductive coupling yields the complex (COD)Pt-(C_2H_4), **12**, which is best characterized as a metallacycle. In the optimized structure (C_2 symmetry) the CC

(29) Yamamoto, T.; Yamamoto, A.; Ikeda, S. *J. Am. Chem. Soc.* **1971**, *93*, 3350−3359, 3360−3363.
(30) Examples: (a) Kohara, T.; Yamamoto, T.; Yamamoto, A. *J. Organomet. Chem.* **1980**, *192*, 265−274. (b) Semmelhack, M. F.; Ryono, L. S. *J. Am. Chem. Soc.* **1975**, *97*, 3873−3875. (c) Yamamoto, T.; Abla, M. *J. Organomet. Chem.* **1997**, *535*, 209−211.
(31) Tatsumi, K.; Nakamura, A.; Komiya, S.; Yamamoto, A.; Yamamoto, T. *J. Am. Chem. Soc.* **1984**, *106*, 8181−8188.

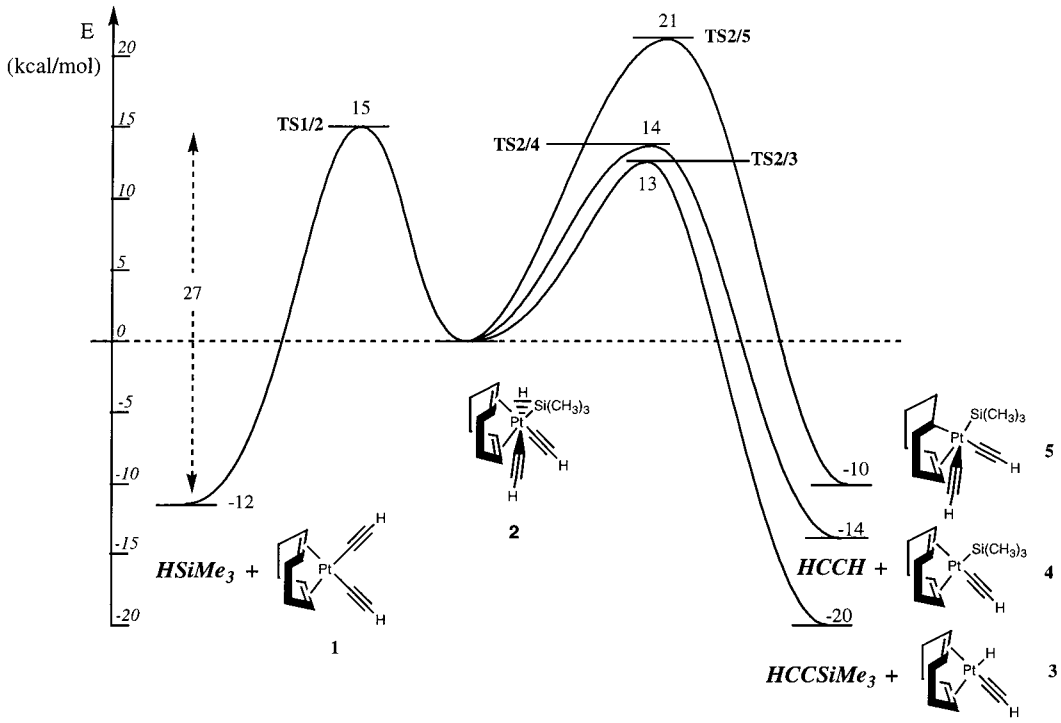

Figure 1. Calculated energy profile for conversion of precatalyst by oxidative addition of trimethylsilane: initial steps (see Scheme 2).

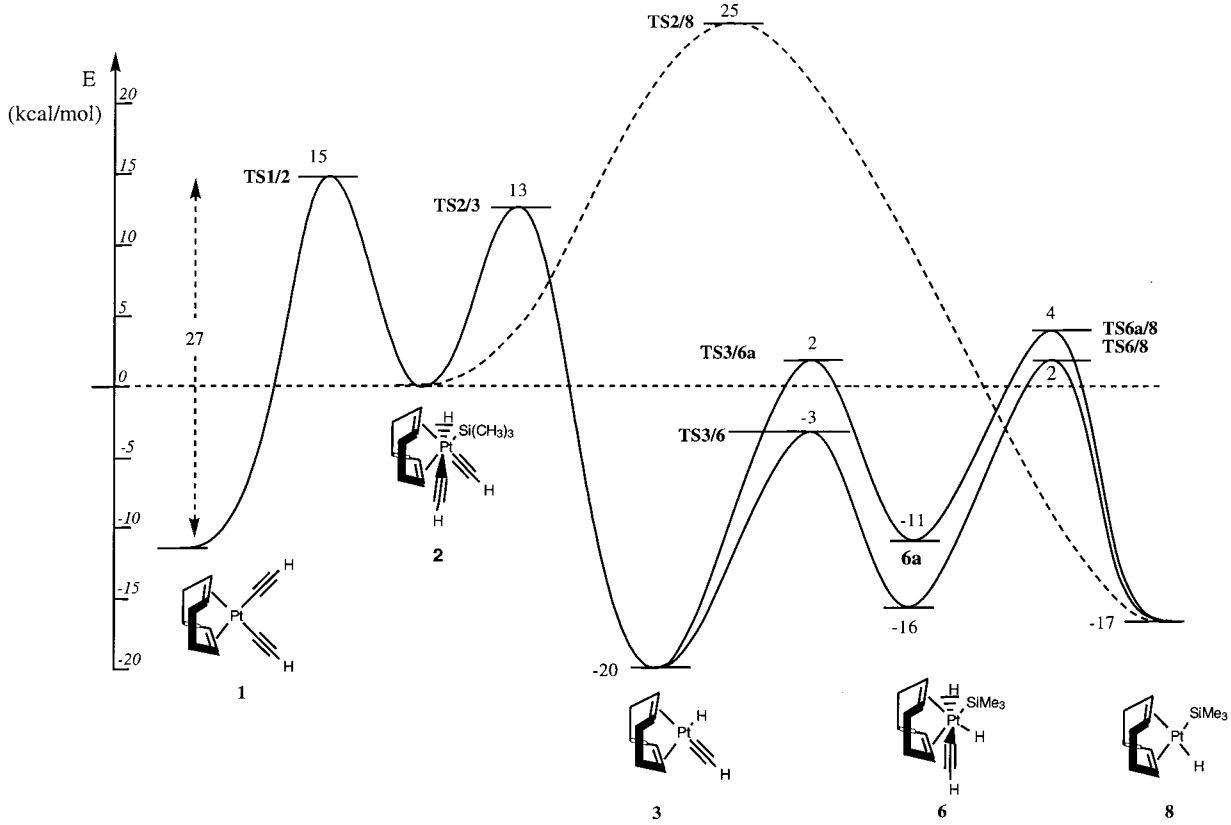

Figure 2. Calculated energy profile for conversion of precatalyst by oxidative addition of trimethylsilane: overview (see Scheme 2).

bond of the C_2H_4 moiety lies in the coordination plane of platinum, the Pt−C bonds in the three-membered ring are quite short (2.11 Å), and the C−C bond in the ring is rather long (1.45 Å). By contrast, in the π complexes studied (**11**, **13**, **19**, **19a**; see Scheme 5), the CC bond of ethylene tends to be perpendicular to the coordination plane of platinum, the Pt−C distances to the C_2H_4 ligand are longer (typically 2.25 Å), and the CC bond in C_2H_4 is shorter (around 1.40 Å). These differences are consistent with the commonly accepted distinction between the σ- and π-bonding mode of olefins.[32]

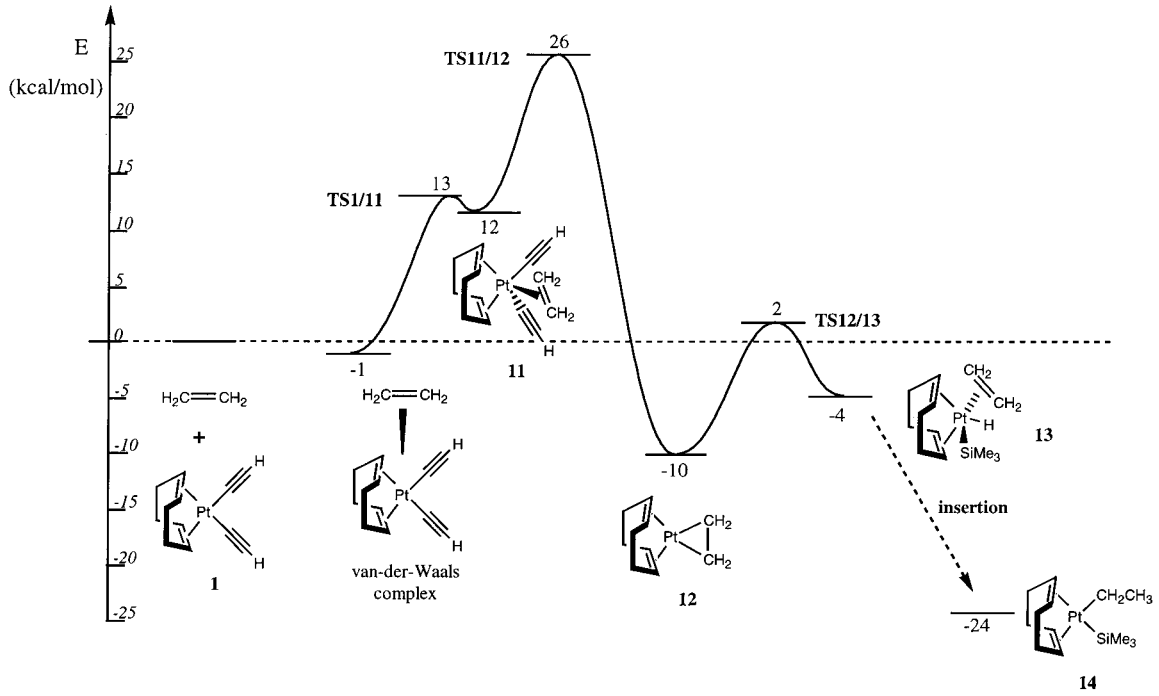

Figure 3. Calculated energy profile for conversion of precatalyst by ethylene coordination and subsequent reactions (see Scheme 4).

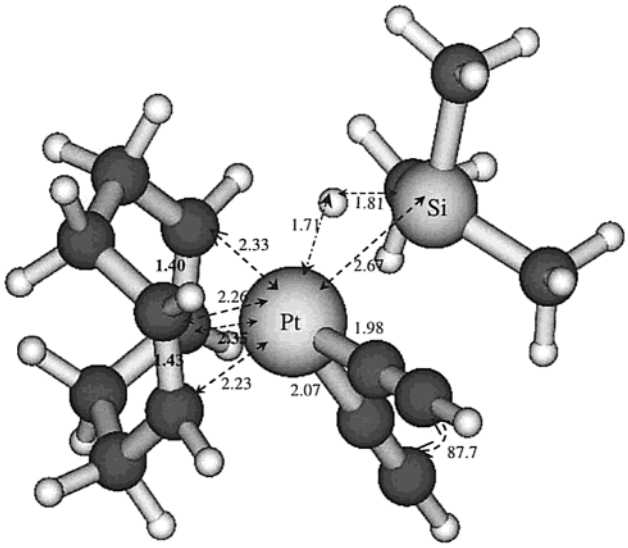

Figure 4. Transition structure for oxidative addition: **1** + $HSiMe_3$ → **2** (bond lengths in Å, bond angles in deg).

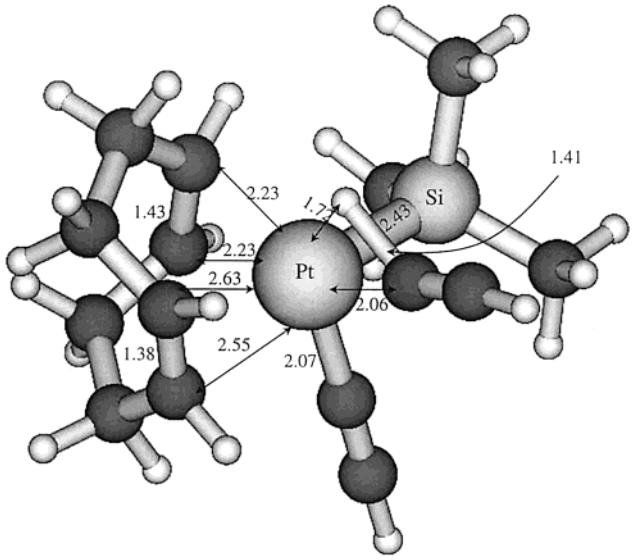

Figure 5. Transition structure for reductive elimination: **2** → **4** + HCCH (bond lengths in Å).

The formation of the metallacycle **12** is exothermic overall (by 10 kcal/mol relative to the separated reactants). The subsequent oxidative addition of $HSiMe_3$ to yield the pentacoordinated complex **13** is facile and requires an activation of only 12 kcal/mol. The corresponding transition structure (see Figure 11) has rather normal Pt−COD distances and clearly moves toward the product geometry in the three-membered ring (Pt−C 2.17 Å, 2.21 Å) and in the reactive region (Pt−Si 2.85 Å, Pt−H 1.78 Å, and Si−H 1.63 Å). The adduct (COD)-Pt(H)$SiMe_3$(C_2H_4), **13**, is an entry point to the Chalk−Harrod cycle (see Scheme 1), which will then continue by insertion of C_2H_4 into the Pt−H bond to form (COD)-Pt($SiMe_3$)(C_2H_5), **14**. Both **13** and **14** are more stable than the separated reactants (by 4 and 24 kcal/mol, respectively).

Looking at the overall energy profile for the reactions in Scheme 4 (see Figure 3), it is clear that the π complex **11** will not be relevant mechanistically because it resides in a very shallow minimum. The rate-limiting barrier for entering the Chalk−Harrod cycle via Scheme 4 amounts to 26 kcal/mol and refers to the conversion **1** → **12** by reductive coupling.

Our calculations thus suggest two different pathways for the activation of the precatalyst **1** that have almost the same effective barriers. In both cases, the initial reaction of the precatalyst corresponds to the rate-

(32) Hartley, F. R. In *Comprehensive Organometallic Chemistry*; Wilkinson, G., Stone, F. G. A., Abel, W. E., Eds.; Pergamon Press: Oxford, 1982; Vol. 6, pp 614−680.

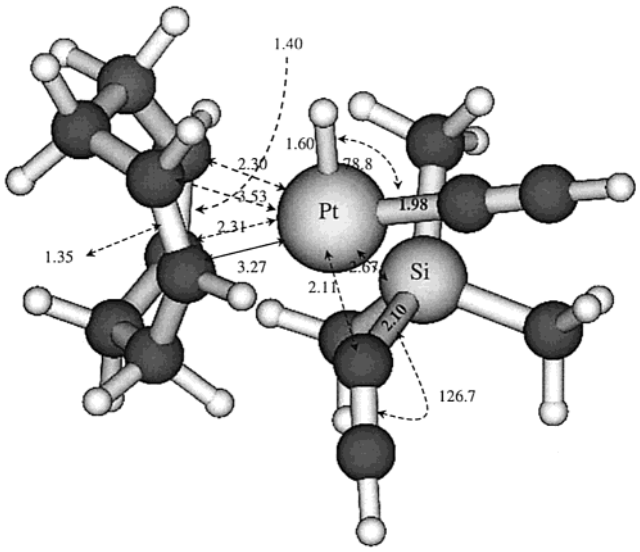

Figure 6. Transition structure for reductive elimination: **2** → **3** + $HCCSiMe_3$ (bond lengths in Å, bond angles in deg).

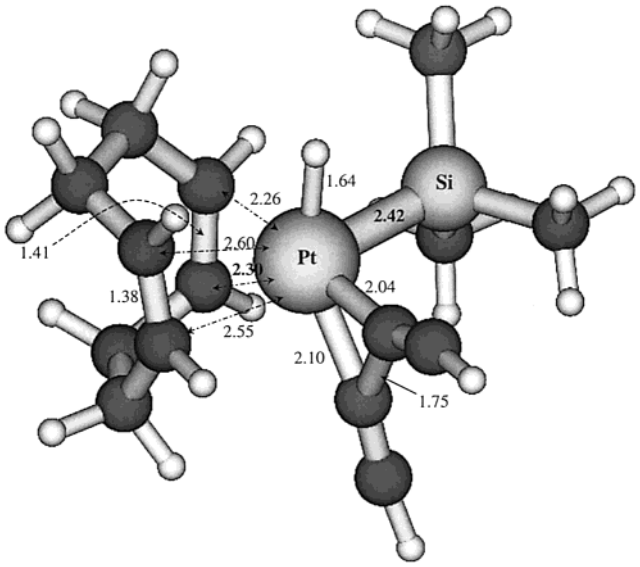

Figure 7. Transition structure for reductive elimination: **2** → **8** + HCCCCH (bond lengths in Å).

determining step: either oxidative addition of $HSiMe_3$ (Scheme 2 and Figure 1, barrier of 26.8 kcal/mol) or coordination of ethylene inducing reductive elimination of diacetylene (Scheme 4 and Figure 3, barrier of 26.4 kcal/mol).

Having completed the discussion of the reactions in Schemes 2−4, we briefly address some thermochemical aspects. Table 3 collects computed dissociation energies for the platinum complexes studied. These energies refer to the following reactions: decoordination of COD (breaking of two π bonds), loss of ethylene from a metallacycle (breaking of two σ bonds in **12** and **17**) or from a π complex (breaking of one π bond in **11**, **13**, and **19**), and reductive elimination of HCCCCH or $HSiMe_3$ (breaking of two σ bonds). It is obvious that the dicoordinated platinum complexes show the highest dissociation energies (55−83 kcal/mol), indicating that the electronic structure of the metal can adapt to the ligands in an optimum manner in this case. By contrast, in the pentacoordinated and hexacoordinated species,

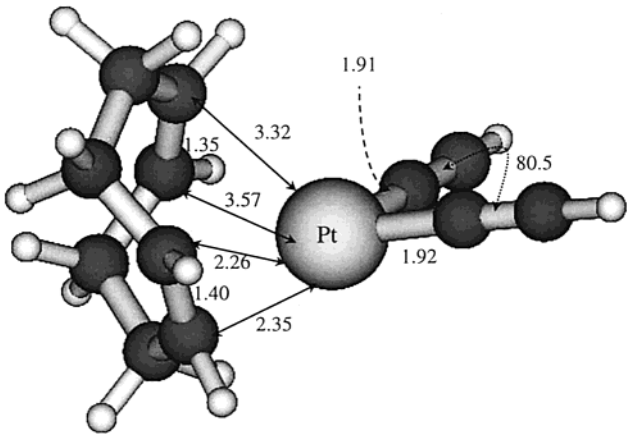

Figure 8. Transition structure for first step of diene decoordination: **1** → **9** (bond lengths in Å, bond angles in deg).

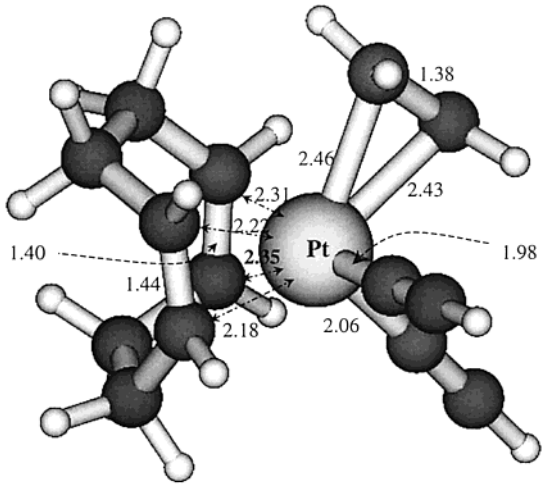

Figure 9. Transition structure for ethylene coordination: **1** + C_2H_4 → **11** (bond lengths in Å).

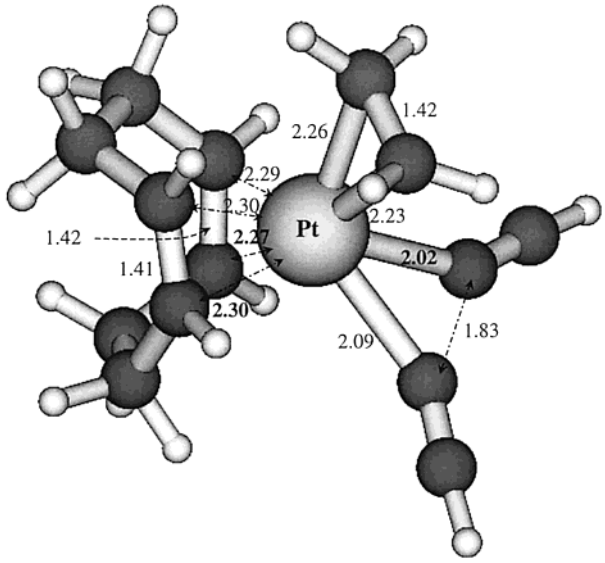

Figure 10. Transition structure for reductive coupling: **11** → **12** + HCCCCH (bond lengths in Å).

only the COD ligand is still weakly bound (by 7−16 kcal/mol), while the loss of the other ligands is exothermic (by 5−22 kcal/mol in the case of the reductive eliminations); this is probably due to the relief of steric

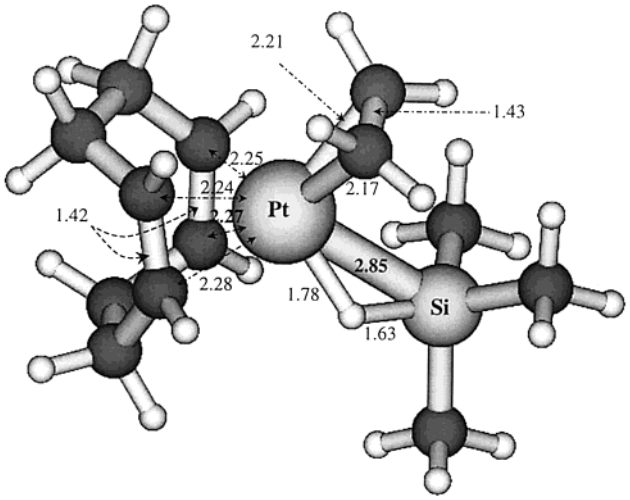

Figure 11. Transition structure for oxidative addition: **12** + $HSiMe_3$ → **13** (bond lengths in Å).

congestion upon dissociation, and partly also to electronic effects.

When comparing different dissociation channels for a given complex, the reductive elimination of diacetylene is normally favored thermodynamically (least endothermic for **1**, **19**, and **20**; most exothermic for **11** and nearly so for **2**). This does not mean, of course, that this reaction is most facile: both for **2** and **11**, there are thermodynamically less favorable channels with smaller barriers (see Figures 2 and 3).

Finally, it is evident that the dissociation energies for ethylene are significantly higher for the metallacycles (**17** and **12**) than for the π complexes (**11**, **13**, and **19**). The difference is seen most clearly for $(COD)Pt(C_2H_4)$, **12**, and $Pt(CCH)_2(C_2H_4)$, **19**, since two more coordination sites are occupied in each case: the corresponding ethylene binding energies are 55 and 33 kcal/mol, respectively. The π complex $Pt(CCH)_2(C_2H_4)$ is related to the precatalyst $(COD)Pt(CCH)_2$ in that the ethylene ligand of **19** replaces the COD ligand of **1** (occupying one of the coordination sites of the COD double bonds). The ethylene binding energy of 33 kcal/mol in **19** is consistent with the energy of 38 kcal/mol needed to decoordinate one COD double bond of **1** (reaction **1** → **9**, see Table 1); the latter value is somewhat higher probably because of the internal strain of COD in **9**. In the tricoordinated complex **19**, the ethylene ligand can easily migrate to the vacant site in the coordination plane of platinum (via a C_{2v} transition state **19a**, barrier of 7 kcal/mol).

Discussion

The relevance of the theoretical results reported in the preceding section is limited by the use of model systems and by the error margins of the DFT calculations. Concerning the latter, the application of gradient-corrected density functionals (such as BP86) in combination with medium-size basis sets and effective core potentials has become an established tool in computational transition metal chemistry over the past years. A comprehensive assessment of this field can be found in a recent issue of *Chemical Reviews*,[33] which includes articles on reactions of transition metal complexes[34] and on palladium and platinum molecular chemistry.[35] These reviews[33−35] complement previous surveys and validation studies for the BP86 functional.[36−38] In the current context, specific comparisons between the results at different theoretical (ab initio and DFT) levels are available for the bis(phosphine)platinum(0)-catalyzed hydrosilylation of ethylene[16−18] and for the ethylene binding energy in $(PH_3)_2Pt(C_2H_4)$.[39,40] On the basis of this material[16−18,33−40] we expect that the chosen theoretical approach will provide realistic results, without claiming quantitative accuracy.

We refrain from making more precise error estimates because the use of model systems introduces an additional uncertainty that is hard to quantify. The real systems contain organopolysiloxanes with Si−H bonds and C═C double bonds which are sterically much more demanding than the model reactants ($HSiMe_3$ and $H_2C{=}CH_2$). In addition, the neighboring substituents in the real systems also exert electronic effects: electronegative oxygen atoms next to the Si−H bond should be electron-withdrawing, while silicon atoms next to the C═C bond should be electron-donating (even though the next nearest atoms in the substituents will counteract these trends to some extent). The electronic effects may be expected to lower the rate-determining barriers for the initial oxidative addition **1** → **2** (see Scheme 2) and the initial reductive elimination **1** → **12** (see Scheme 4), respectively. On the other hand, the increased steric demand would tend to increase these barriers since the corresponding transition states are more highly coordinated than the reactants. Hence it is difficult to predict how much the barriers will change when going from the model to the real system. Under these circumstances, we have decided to use the computational results for the model system at face value and to make an attempt to relate them to experimental evidence available for the real systems.

To distinguish between the two modes of activation suggested by the DFT calculations, two substituted siloxanes were heated in the presence of the precatalyst $(COD)Pt(CCR)_2$ with R = *p*-trimethylsilylphenyl (**1b**) (see Experimental Section). Pentamethyldisiloxane $Me_3Si{-}O{-}SiHMe_2$ was found to react already at 60 °C, and tempering at 120 °C for 1 h led to a complex mixture of products including COD, cyclooctene, $R{-}C_2H_5$, and a resin of unidentified composition. By contrast, the divinyl-substituted polysiloxane $(CH_2{=}CH)SiMe_2{-}O{-}[SiMe_2{-}O]_{20}{-}SiMe_2(CH{=}CH_2)$ could be heated to 120 °C for 1 h without any signs of a reaction; in particular, no diacetylene product could be detected. These experiments indicate that the vinyl group in a polysiloxane is less reactive toward the precatalyst than the Si−H group, implying that the initial activation of the precatalyst should involve the oxidative addition of an Si−H bond. It should also be noted in this context that the reported reductive eliminations in dialkyl(dipyridyl)-

(33) Davidson, E. R., Ed. *Chem. Rev.* **2000**, *100*, 351−818.
(34) Niu, S.; Hall, M. B. *Chem. Rev.* **2000**, *100*, 353−406.
(35) Dedieu, A. *Chem. Rev.* **2000**, *100*, 543−600.
(36) Ziegler, T. *Chem. Rev.* **1991**, *91*, 651−667.
(37) Ziegler, T. *Can. J. Chem.* **1995**, *73*, 743−761.
(38) Jonas, V.; Thiel, W. *J. Chem. Phys.* **1995**, *102*, 8474−8484.
(39) Uddin, J.; Dapprich, S.; Frenking, G.; Yates, B. F. *Organometallics* **1999**, *18*, 457−465.
(40) Yates, B. F. *J. Mol. Struct.* (*THEOCHEM*) **2000**, *506*, 223−232.

Table 2. Optimized Bond Lengths (Å) in Selected Platinum Complexes (see Scheme 5)

bond[a,b] (ligand)	Pt−C1 (COD)	Pt−C2 (COD)	Pt−C3 (COD)	Pt−C4 (COD)	C1═C2 (COD)	C3═C4 (COD)	Pt−C5 (CCH)	Pt−C6 (CCH)	Pt−H	Pt−Si	Pt−C7 (C_2H_4)	Pt−C8 (C_2H_4)	C7═C8 (C_2H_4)
1	2.25	2.28	2.28	2.25	1.40	1.40	1.97	1.97					
2	2.32	2.30	2.59[c]	2.65[c]	1.40	1.37	1.99[e]	2.08[d]	1.62	2.43			
2a	2.29	2.32	2.37[d]	2.36[d]	1.41	1.40	2.00[e]	2.10[c]	1.58	2.54			
2b	2.48[d]	2.49[d]	2.79[c]	2.70[c]	1.38	1.37	2.03	2.03	1.57	2.42			
2c	2.28	2.28	2.30	2.27	1.41	1.41	2.00	2.00	1.66[c]	2.59[d]			
3	2.22	2.24	2.35[d]	2.31[d]	1.41	1.38	1.97		1.59	-			
4	2.21	2.24	2.50[c]	2.43[c]	1.41	1.38	1.98			2.39			
5	2.99	2.13[f]	2.38	2.30	1.55	1.40	1.96	2.07		2.44			
6	2.34[d]	2.38[d]	2.57[c]	2.53[c]	1.40	1.38	2.07		1.58[g]	2.40			
6a	2.26	2.27	2.53[c]	2.47[c]	1.41	1.38	1.99		1.65[h]	2.42			
7	2.56[c]	2.60[c]	2.64[c]	2.55[c]	1.38	1.38	2.06		1.63	2.41[i]			
8	2.26[d]	2.29[d]	2.44[c]	2.37[c]	1.40	1.39			1.61	2.38			
9	3.65	3.97	2.24	2.38	1.35	1.40	1.93[e]	1.91					
11	2.23	2.21	2.33	2.33	1.43	1.40	1.98[e]	2.08			2.29	2.24	1.41
12	2.30	2.27	2.27	2.30	1.40	1.40					2.11	2.11	1.45
13	2.28	2.33	2.28	2.22	1.41	1.43			1.60	2.47	2.28	2.23	1.42
14	2.47[c]	2.38[d]	2.26	2.29	1.38	1.40				2.39	2.10[j]		

[a] C1, C2, C3, C4: unsaturated carbon atoms of COD (see Scheme 5: C1 and C2 upper double bond, C1 and C3 frontside atoms); C5, C6: carbon atoms of ethynyl group; C7, C8: carbon atoms of ethylene moiety. [b] The CC triple bond lengths in the ethynyl group are not given since they are almost constant (1.23 Å). [c] Trans to $SiMe_3$. [d] Trans to H. [e] Trans to one of the COD double bonds. [f] σ-bonded to Pt. [g] Second Pt−H bond trans to CCH: 1.63 Å. [h] Same value for both Pt−H bonds (difference of 0.002 Å). [i] Same value for both Pt−Si bonds (difference of 0.003 Å). [j] Pt−C(ethyl).

Table 3. Calculated Dissociation Energies (kcal/mol)[a,b]

complex	label	coord[c]	ox[d]	loss of	ΔE[e]
Pt(COD)	**15**	2	0	COD	71.2
$Pt(CCH)_2$	**16**	2	2	HCCCCH	54.7
$Pt(C_2H_4)$	**17**	2	2	C_2H_4	75.8
$Pt(H)SiMe_3$	**18**	2	2	$HSiMe_3$	82.5
$Pt(CCH)_2(C_2H_4)$	**19**	3	2	C_2H_4	33.0
				HCCCCH	11.9
$Pt(CCH)_2(H)SiMe_3$	**20**	4	4	$HSiMe_3$	38.9
				HCCCCH	11.1
$(COD)Pt(CCH)_2$	**1**	4	2	COD	61.2
				HCCCCH	44.7
$(COD)Pt(C_2H_4)$	**12**	4	2	COD	50.0
				C_2H_4	54.6
$(COD)Pt(H)SiMe_3$	**8**	4	2	COD	38.0
				$HSiMe_3$	49.3
$(COD)Pt(CCH)_2(H)SiMe_3$	**2**	6	4	COD	10.5
				$HSiMe_3$	−11.8
				HCCH	−14.1
				HCCCCH	−16.5
				$HCCSiMe_3$	−19.9
$(COD)Pt(C_2H_4)(CCH)_2$	**11**	5	2	COD	16.2
				C_2H_4	−12.0
				HCCCCH	−22.0
$(COD)Pt(C_2H_4)(H)SiMe_3$	**13**	5	2	COD	7.3
				C_2H_4	−0.3
				$HSiMe_3$	−5.6

[a] Computed from the total energies given in Table S1 of Supporting Information; zero-point vibrational corrections are not included. [b] Judging from the calculated geometries and energies, the ethylene ligand forms a metallacycle in two cases (**12**, **17**) and a π complex in the other cases (**11**, **13**, **19**). The coordination and oxidation numbers are assigned accordingly. [c] Coordination number of Pt. [d] Formal oxidation number of Pt. [e] Negative values indicate exothermic dissociation.

nickel complexes[29,30] are activated by olefins with electron-withdrawing substituents.

Kinetic measurements were carried out for an unsaturated polysiloxane using three different precatalysts $(COD)Pt(CCR)_2$ with R = phenyl (**1a**), R = *p*-trimethylsilylphenyl (**1b**), and R = pentafluorophenyl (**1c**) (see Experimental Section). The resulting Arrhenius activation energies are 29.5, 26.6, and 25.4 kcal/mol, respectively. These values are close to the computed barrier of 26.8 kcal/mol (see Table 1) for the initial oxidative addition **1** + $HSiMe_3$ → **2** in the model system with R = H (**1**). For further comparison, additional calculations were done on this reaction using the precatalysts **1a**, **1b**, and **1c**. In the case of R = phenyl (**1a**), full geometry optimizations were performed as well as single-point calculations which employed the optimized structures of the parent system, except for replacement of the substituent R = H in the ethynyl groups by R = Ph (standard bond lengths and angles): both approaches led to the same[41] activation energy of 28.2 kcal/mol for **1a**. In the case of **1b** and **1c**, only the less expensive single-point calculations were carried out, yielding barriers of 28.0 and 26.5 kcal/mol, respectively. It is evident that the computed DFT barriers for **1a**−**c** are consistent with the experimental data with regard to both the barrier heights and the substituent effects encountered. This supports the notion that the precatalysts under study are indeed activated by the initial oxidative addition of a silane.

Conclusions

The DFT calculations on a model system provide two plausible pathways for the activation of precatalyst **1** (see Schemes 2 and 4, Figures 1−3). The first one involves a sequence of four oxidative additions and reductive eliminations to gain access to the Chalk−Harrod cycle, while the second one accomplishes this goal more directly by a reductive coupling that is induced by olefin coordination. In both cases, the initial step is rate-determining, with a computed barrier of 27 kcal/mol. The available experimental evidence for the real polysiloxane systems favors the first pathway. Therefore we propose that the activation of the precatalysts $(COD)Pt(CCR)_2$ is initiated by oxidative addition of Si−H. The corresponding barrier, and hence the kick-off temperature of the catalyst, can be tuned by proper choice of the substituent R in the alkynyl groups.

Experimental Section

All experiments were conducted in a dry nitrogen atmosphere using standard Schlenk techniques. Solvents and

(41) Test calculations with other small substituents R show that the barriers from single-point calculations and from full optimizations normally differ somewhat (by about 0.5 kcal/mol).

phenylacetylene were obtained from Aldrich and used without further purification. The compounds were characterized by a combination of elemental analysis and spectroscopic methods. C and H analyses were determined with a Leco-CHN 800 microanalyzer. Infrared spectra (range 400−4000 cm^{-1}) were recorded as KBr disks on a Nicolet Magna System 750. ^1H and ^{13}C NMR spectra were recorded in $CDCl_3$ solution on Bruker Advance DPX 360 (^1H, 360.13 MHz) and DPX 400 (^{13}C, 100.62 MHz) machines. The starting material $(COD)PtCl_2$ was prepared as described in the literature.[42]

(COD)Pt(C≡CPh)$_2$ (1a). The synthesis followed published procedures.[43] IR: ν(C≡C) 2124 (s). ^1H NMR: δ 7.38−7.10 (m, 5 H, ArH), 5.68 (t, 4 H, $^2J_{HPt}$ = 45 Hz, CH=CH), 2.55 (br s, 8 H, CH_2). ^{13}C NMR: phenyl, 121.1 (*C*−C≡C), 132.3 ((*C*H)$_2$C−), 128.2 ((*C*H−CH)$_2$C−), 126.8 ((CH)$_2$*C*H), COD, 30.8 (*C*H$_2$), 104.6 (*C*H); others, 94.9 (Pt−*C*≡), 108.8 (Pt−C≡*C*−). Anal. Calcd for $C_{24}H_{22}Pt$: C, 57.0; H, 4.4. Found: C, 56.7; H, 4.4.

(COD)Pt(C≡C−C$_6$H$_4$SiMe$_3$-p)$_2$ (1b).[44] A suspension of 0.50 g of $(COD)PtCl_2$ in 20 mL of methanol was cooled to −20 °C. A freshly prepared solution of 0.77 g of (*p*-trimethylsilylphenylethynyl)trimethylsilane[45] and sodium methanolate (61.5 mg of sodium, 15 mL of methanol) was then slowly added dropwise. After 20 min, the mixture was heated to room temperature, and the precipitate was filtered off and washed five times with acetone. Yield: 0.78 g (90%). IR: ν(C≡C) 2124 (s). ^1H NMR: δ 7.36 (s, 8 H, ArH), 5.68 (br t, 4 H, $^2J_{HPt}$ = 44 Hz, CH=CH), 2.55 (br s, 8 H, CH_2), 0.20 (s, 18 H, Si(CH$_3$)$_3$). ^{13}C NMR: aryl group, 126.5 (*C*−C≡C), 130.5 ((*C*H)$_2$C−), 132.5 ((*C*H−CH)$_2$C−), 138.0 ((CH)$_2$*C*−Si(CH$_3$)$_3$); COD, 30.0 (*C*H$_2$), 103.8 (*C*H); others, 94.8 (Pt−*C*≡), 108.2 (Pt−C≡*C*−), −1.5 (Si(*C*H$_3$)$_3$). Anal. Calcd for $C_{30}H_{38}Si_2Pt$: C, 55.5; H, 5.9. Found: C, 54.8; H, 5.9.

(COD)Pt(C≡C−C$_6$F$_5$)$_2$ (1c).[46] A suspension of 2.0 g (5.35 mmol) of $(COD)PtCl_2$ in 30 mL of methanol was cooled to −30 °C. A freshly prepared solution of 2.21 g (11.5 mmol) of (pentafluorophenyl)acetylene[47] was added to this suspension followed by 12.75 mL (10.0 mmol) of sodium methanolate (0.784 M in methanol). After 60 min at −30 °C, the mixture was allowed to warm to room temperature, and the precipitate was filtered off and washed five times with acetone. Yield: 3.20 g (87%). IR: ν(C≡C) 2143 (m). ^1H NMR: δ 5.66 (t, 4 H, $^2J_{HPt}$ = 40.5 Hz, CH=CH), 2.55 (s, 8 H, CH_2), 2.50 (s, 6 H, CH_3). Anal. Calcd for $C_{24}H_{12}F_{10}Pt$: C, 42.1; H, 1.8. Found: C, 41.6; H, 1.7.

Siloxane Compounds for Kinetic Studies. The SiH cross-linking agent was a copolymer containing Me_3SiO, Me_2SiO, and MeHSiO units, with a viscosity of 310 mPa·s and a weight content of 0.46% of Si-bonded hydrogen; 12.0 g of this cross-linker was mixed with 200.0 g of a poly(dimethylsiloxane) terminated at both ends with a vinyl group (viscosity 1000 mPa·s) and 4.24 mg of 1-ethynyl-1-cyclohexanol. Thereafter, a solution of the platin compound in 3 mL of CH_2Cl_2 was added and mixed homogeneously. The platinum content in the mixture was chosen as 10 ppm, corresponding to 5.5 mg of **1a**, 7.1 mg of **1b**, and 7.5 mg of **1c**.

Kinetic Studies. Measurements were done at seven temperatures between 75 and 90 °C. The curing times were determined at each temperature using a gel timer (following DIN 1694). After completing a series of consecutive measurements at different temperatures, the curing time was determined again at the initial temperature which reproduced the initially measured value to within 5% and thereby confirmed the stability of the silicone mixture during these experiments.

Reactivity Studies for 1b. A mixture of 4.0 g of a vinyldimethylsilyloxy-terminated polysiloxane (CH_2=CH)-$SiMe_2$−O−[$SiMe_2$−O]$_{20}$−$SiMe_2$(CH=CH_2) and 2.0 g of **1b** was stored at 120 °C for 1 h, but no reaction occurred (neither in air nor in a vacuum). Likewise, a mixture of 4.0 g of pentamethyldisiloxane Me_3Si−O−$SiHMe_2$ and 2.0 g of **1b** was stored at 120 °C for 1 h; in this case, a reaction took place. The reaction mixture was analyzed by NMR, IR, and GC: cyclooctadiene, cyclooctene, and (*p*-ethylphenyl)trimethylsilane could be identified as reaction products, along with a dark brown resin of unknown composition (no ethynyl groups left according to IR).

Acknowledgment. We thank Prof. P. W. Jolly for pointing out previous experimental work on reductive coupling in nickel complexes and for suggesting analogous calculations in our system. We are also grateful to Dr. F. Achenbach, Dr. V. Frey, Dr. O. Schäfer, and Dr. W. Schmitt-Sody for many helpful discussions, and to Debasis Koley for his help in the final stage of the computational work.

Supporting Information Available: Total energies without and with zero-point vibrational corrections of all relevant species (Table S1), further optimized bond lengths and angles (Table S2), and additional transition structures (Figures S1−S4). This material is available free of charge via the Internet at http://pubs.acs.org.

OM0200196

(42) McDermott, J. X.; White, J. W.; Whitesides, G. M. *J. Am. Chem. Soc.* **1976**, *98*, 6521−6528.
(43) Cross, R. J.; Davidson, M. F. *J. Chem. Soc., Dalton Trans.* **1986**, 1987−1992.
(44) Achenbach, F.; Fehn, A. DE 19,938,338, 1999.
(45) Eaborn, C.; Thompson, A. R.; Walton, D. R. M. *J. Chem. Soc. (C)* **1967**, 1364−1366.
(46) (a) Achenbach, F.; Fehn, A. DE 19,847,097, 1998. (b) Achenbach, F.; Fehn, A. Eur. Pat. Appl. 994,159, 1998.
(47) Waugh, F.; Walton, D. R. M. *J. Organomet. Chem.* **1972**, *39*, 275−278.